Chemistry & Biology
Article

Hydrophobic Amino Acid and Single-Atom Substitutions Increase DNA Polymerase Selectivity

Nicolas Z. Rudinger,[1] Ramon Kranaster,[1] and Andreas Marx[1,*]
[1] Department of Chemistry, University of Konstanz, Universitätsstrasse 10, 78457 Konstanz, Germany
*Correspondence: andreas.marx@uni-konstanz.de
DOI 10.1016/j.chembiol.2006.11.016

SUMMARY

DNA polymerase fidelity is of immense biological importance due to the fundamental requirement for accurate DNA synthesis in both replicative and repair processes. Subtle hydrogen-bonding networks between DNA polymerases and their primer/template substrates are believed to have impact on DNA polymerase selectivity. We show that deleting defined interactions of that kind by rationally designed hydrophobic substitution mutations can result in a more selective enzyme. Furthermore, a single-atom replacement within the DNA substrate through chemical modification, which leads to an altered acceptor potential and steric demand of the DNA substrate, further increased the selectivity of the developed systems. Accordingly, this study about the impact of hydrophobic alterations on DNA polymerase selectivity—enzyme and substrate wise—further highlights the relevance of shape complementary and polar interactions on DNA polymerase selectivity.

INTRODUCTION

DNA polymerase fidelity is essential for the integrity of the genome of every living species. The fidelity of DNA polymerase catalysis is thus an important determinant of the evolution of species and the origin of human diseases [1]. The selectivity of nucleotide insertion during DNA replication is believed to be achieved by editing of nucleotide geometry within a tight binding pocket [2–7]. Depending on the DNA polymerase, insertion of noncanonical nucleotides occurs to varied extent. Nevertheless, misinsertion results in a nucleobase substitution only if a mismatched primer terminus is extended efficiently without being proofread. Thus, discrimination of a DNA polymerase to efficiently extend mismatches is a critical determinant for overall DNA replication fidelity [2–7]. Contacts of the DNA polymerase with the minor groove of the primer/template duplex have been cited as important factors in achieving DNA polymerase mismatch extension selectivity [2–7]. Extensive biochemical investigations on DNA polymerase/substrate interactions have been performed, involving mutation studies [8–12] as well as the application of chemically modified nucleoside probes [11, 13, 14]. These studies suggest that such interactions may indeed function as sensor for the detection of mismatches in the primer/template through presentation of aberrant acceptor patterns by the mispairs. DNA polymerases exhibiting higher fidelity mainly interact with the minor groove through specific hydrogen bonds with the N-3 atoms of purines and O-2 atoms of pyrimidines as acceptors [15–22].

In this context, it has been suggested that motif C plays a key role not only in enabling catalysis but also to function in a common mechanism of mismatch recognition in the primer/template [16]. It is believed that minor groove hydrogen bonding of motif C residues to the second primer nucleobase in A family and B family DNA polymerases contributes to mismatch sensing (Figure 1A) [15, 16, 18–21]. These interactions persist sequence independently as long as the nucleobase pair has proper Watson-Crick geometry [16, 23]. Motif C is a highly conserved sequence in DNA polymerases [2–7, 16, 24]. This high conservation could also reflect additional and central functions of this motif. It was found for family A DNA polymerases (e.g., *E. coli* DNA polymerase I, *Thermus aquatiqus* DNA polymerase) that hydrophobic substitutions in motif C result in enzymes that exhibit increased mismatch extension selectivity [25, 26]. These findings suggest involvement of motif C residues in extension selectivity of family B DNA polymerases as well. However, the sequences of motif C, e.g., in family A and B DNA polymerases, significantly differ [16, 27, 28]. For family B DNA polymerases, a different, albeit related, polar interaction comprising an aspartate and lysine is believed to contact the DNA minor groove (Figure 1A) [16]. The respective amino acids are located in the YGDTDS and KXY motifs that are highly conserved among family B DNA polymerases from eukaryotic, bacterial, and viral origins (Figure 1B) [29, 30]. Nevertheless, the function of this interaction in family B DNA polymerase mediated synthesis has not been investigated. Here, we report on the impact of rationally designed hydrophobic substitution mutations on the depicted interaction of motif C with the primer/template in a family B DNA polymerase. We find that deleting the defined polar interaction by hydrophobic substitution mutations can result in a more selective enzyme. To our knowledge, this is the first time that the selectivity of an already

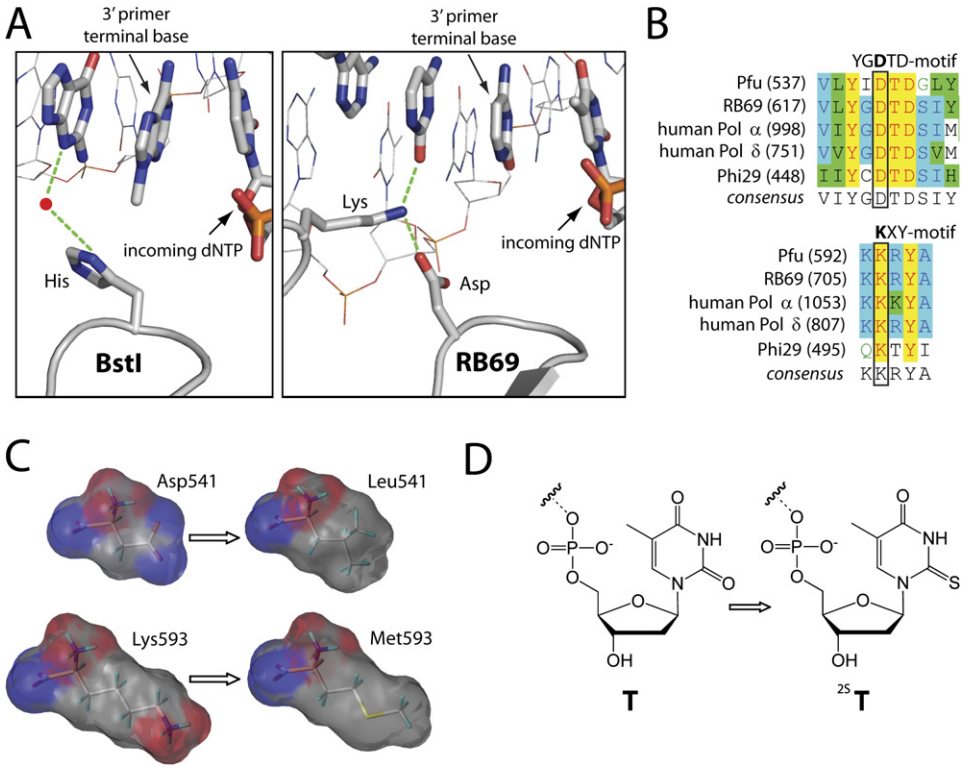

Figure 1. Design of Mutations and Chemical Modifications

(A) Minor groove interactions of motif C in family A and B DNA polymerases represented by *Bst*I (PDB code 2BDP) [19] and RB69 (PDB code 1IG9) [16] DNA polymerase ternary complexes, respectively. For clarity, the sugar-phosphate backbone for the primer strand is not depicted.

(B) Amino acid sequence alignments of motifs YG(D)TD and (K)XY in family B DNA polymerases. Rectangles highlight positions chosen for mutagenesis in *Pfu* DNA polymerase.

(C) Connolly surfaces showing the hydrogen-bonding capability of wild-type and mutant residues. Amino acid numbers define positions for *Pfu* DNA polymerase. Red surfaces display H-bonding acceptors, and blue surfaces H-bonding donors.

(D) Chemical structures of thymidine and 2-thiothymidine.

high-fidelity family B DNA polymerase was increased. Additionally, single-atom replacement within the DNA substrate through chemical modification further increased selectivity of the DNA polymerases described herein. Accordingly, this study about the impact of modifications on DNA polymerase selectivity—enzyme- and substrate-wise—indicates that in addition to shape, attenuation of hydrogen-bonding capability can increase selectivity.

RESULTS

Rational Design of Biological and Chemical Alterations—Structural Determinants

As target for our study, we chose the widely applied high-fidelity *Pyrococcus furiosus* (*Pfu*) DNA polymerase for mutation and subsequent evaluation [31–33]. In order to minimize steric effects, the hydrophobic amino acid substitutions were designed in a way to be maximal isosteric. Apparently, the DNA polymerase of phage RB69 (RB69) is the sole B family DNA polymerase of which the structure of a ternary complex is available. Amino acid alignments of RB69 and *Pfu* DNA polymerases show that the residues responsible for building the above mentioned salt bridge are highly conserved (Figures 1A and 1B). Thus, at the respective positions in *Pfu* DNA polymerase aspartate was replaced by leucine and lysine by methionine (Figure 1C).

Accordingly, a *Pfu* DNA polymerase single-mutant D541L (henceforth named as "M1") and a double-mutant D541L/K593M (henceforth named as "M2") were constructed and tested. Since we were interested in the intrinsic effects of mutations on key polymerization steps, we employed an exonuclease deficient variant of *Pfu* DNA polymerase. To further access effects of polarity and size of the depicted interaction on primer processing, we altered the acceptor potential and steric demand of the DNA substrate. This was realized by employing primer probes bearing a 2-thiothymidine residue (^{2S}T) (Figure 1D) at the 3′ terminus of the primer strand.

PCR Activity, Specific Activity, and Selectivity

The resulting purified mutants were tested for PCR activity under identical conditions. We found that mutant M1 was incapable of yielding detectable amounts of PCR product of the desired length (Figure 2A). The same results were found for the single-mutant K593M (data not shown). PCR activity is rescued by hydrophobic substitution of

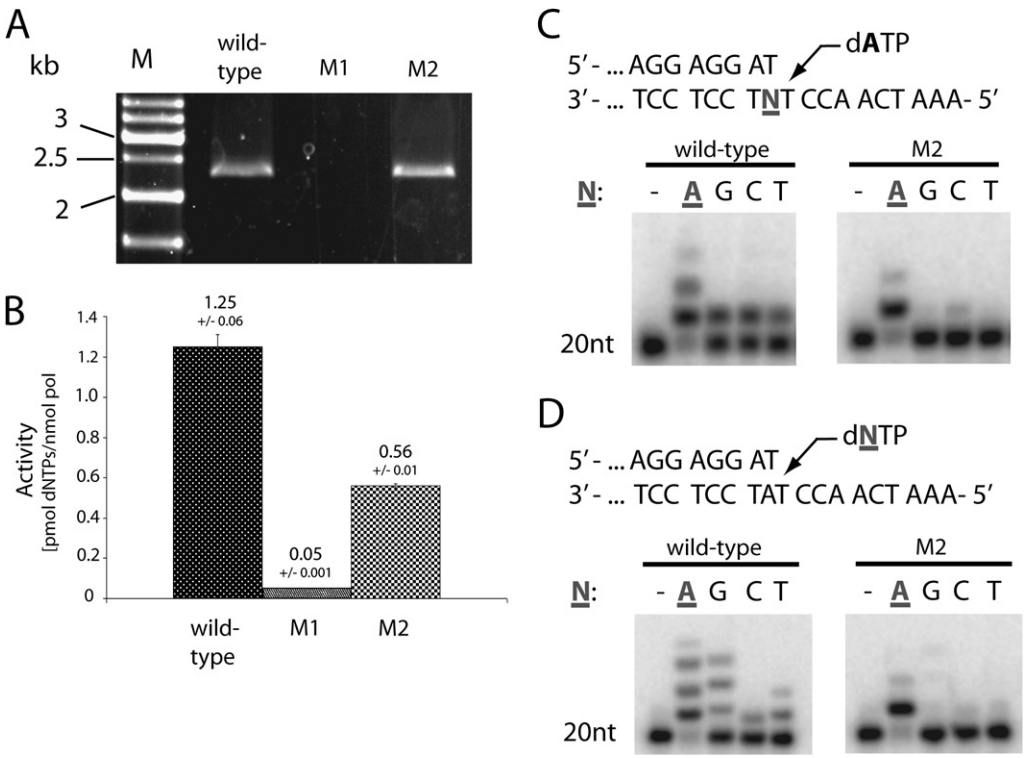

Figure 2. PCR Activity, Specific Activity, Mismatch Extension, and Misinsertion of Wild-Type and Mutant DNA Polymerases

(A) PCR (25 cycles) conducted with equal amounts of the respective enzyme under identical reaction conditions.

(B) Specific activities of the respective enzymes in μmol dNTPs/pmol pol. The presented data derive from averages of independent experiments repeated at least three times.

(C) Mismatch extension studies (with dATP only) conducted with the wild-type and double-mutant (M2) enzyme. Primer/template constructs resulting in matched and mismatched complexes were employed as indicated. The first lane of each set represents a control without enzyme.

(D) Insertion and misinsertion of dNTP (as indicated) conducted with the wild-type and mutant M2. Partial sequences employed are depicted in the figure.

the second amino acid. Quantification of the specific enzyme activity indicates that mutant M2 displays about 50% WT activity, whereas mutant M1 displays less than 4% WT activity (Figure 2B). Next, we qualitatively assayed the wild-type and mutant M2 in their capability to extend from matched and mismatched primers (Figure 2C). These data show that the wild-type enzyme readily extends a mismatch under the chosen conditions. Applying identical conditions to mutant M2 indicates that it has markedly decreased mismatch extension efficiency. Next, we investigated the effects of mismatches located in the primer/template distal to the 3′ primer terminus. We found that the mutant M2 is able to sense mismatches that are located up to four positions upstream of the 3′ primer terminus to a greater extent compared to the wild-type and translate their presence in reduced nucleotide insertion efficiency (Figure 3).

Quantification of the mismatch extension selectivity indicates that mutant M2 is 10-fold more selective in comparison to the wild-type enzyme (Figure 4B). The 2-carbonyl function of thymidines points toward the minor groove and is a potential acceptor of the side chain of K593 in *Pfu* DNA polymerase. When replacing oxygen with sulfur in this position, chemical modification of thymidine results in reduced hydrogen-bonding capability and moderately increased size compared to thymidine [34]. Primers containing the 2-thiothymidine were synthesized as recently described [34] and employed in primer extension studies (Figure 4A). Apparently, the atom substitution in the primer strand results in an increased mismatch extension selectivity of the wild-type enzyme. Noteworthy, primer extension of the mismatched ^{2S}T-primer/template complex by the wild-type is strongly impaired after the penultimate position. Quantification indicates that when employing the chemically modified primer, the wild-type enzyme is 2-fold more selective (Figure 4B). A more pronounced effect was measured for combination of the biological and chemical alterations. Hydrophobic substitution mutations of the enzyme and a single-atom replacement in the primer result in a more than 25-fold increase in mismatch extension selectivity over the wild-type enzyme with natural substrate (Figure 4B). Additionally, the wild-type and mutant enzymes exhibit increased steady-state turnover rates when thiolated primers were employed. Under these conditions, the turnover rate of mutant M2 on a matched primer/template complex is almost doubled

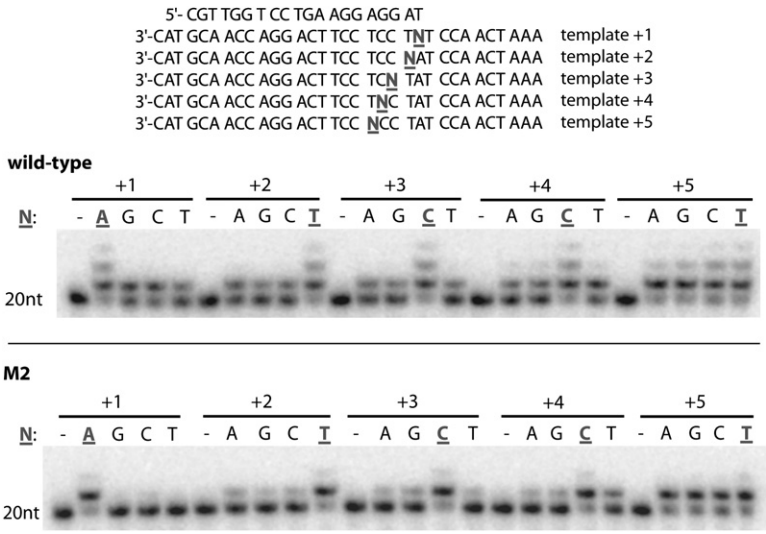

Figure 3. Recognition of Remote Mismatches of Wild-Type and Mutant DNA Polymerases

The first lane of each set represents a control without enzyme. Primer/template constructs resulting in matched and mismatched complexes, located at the 3′-primer terminus or up to four positions upstream. All reactions contained equal amounts of the respective enzyme, dATP, and primer/template complex. Sequences of primer and templates are indicated in the figure. Underlined letters indicate matched cases, nonunderlined indicate mismatched cases. N = A, G, C, or T, as indicated.

and exceeds the wild-type (Figure 4B). Hence, additional activity of mutant M2 is rescued by the 2-thiothymidine modified primer.

Next, we investigated whether mutations impact nucleotide-insertion selectivity. To begin with, data were obtained from qualitative investigation of insertion selectivity first. In contrast to the wild-type, mutant M2 misincorporates noncanonical nucleotides to a lesser extent (Figure 2D). In order to quantitatively probe misinsertion and mismatch extension fidelity, kinetic parameters of the systems created herein were determined. Quantitative steady-state kinetic measurements under single completed hit conditions substantiate the results of the described qualitative misinsertion experiments. The wild-type misinserts dCTP and dGTP with almost equal efficiency and dTTP with higher efficiency (Table 1). Compared to the wild-type, mutant M2 displays a 4-fold increase in misinsertion fidelity in case of dCTP misinsertion opposite to T (Table 1). Furthermore, for mutant M2, no misinsertion was measurable for dGTP and dTTP under the conditions applied. However, the insertion efficiency of mutant M2 in terms of dATP opposite to T is decreased by 2.5-fold (Table 1). Taken together, the mutant enzyme displays higher insertion fidelity compared to the wild-type enzyme as well.

Real-Time PCR Experiments

Next, we investigated whether the increased extension selectivity of M2 persists under conditions routinely employed in PCR and can be carried forward to allele-specific PCR. Thus, we conducted real-time PCR experiments with both the wild-type and mutant M2. The obtained results show that mutant M2 is capable of discriminating a T/G mismatch at the primer terminus, whereas the wild-type is not (Figure 5). A difference of the PCR cycle number of the threshold crossing (ΔC_t) of four to seven between the matched and mismatched primer/template complexes can be detected for mutant M2. This function persists even if the template concentration is lowered by four orders of magnitude (Figure 5B). Accordingly, the enhanced extension fidelity of M2 is apparent under PCR conditions as well and can be carried forward to allele-specific PCR.

DISCUSSION

The results presented in this study show that deletion of a definite polar interaction between polymerase and primer, which is believed to scan the primer strand through the minor groove, results in an enzyme with higher selectivity. Deletion of this interaction was realized by rationally designed replacements of polar residues by hydrophobic amino acids of similar size. Although belonging to the same DNA polymerase family, *Pfu* and RB69 DNA polymerases share a sequence homology of only 16%. Based on structural data of RB69 DNA polymerase, rationally designed mutations were introduced into *Pfu* DNA polymerase. In accordance to previous reports [29, 30] on mutations of the conserved residues Asp and Lys (bold) in motifs YGDTDS and KXY, both single-mutants *Pfu*-D541L and *Pfu*-K593M are strongly impaired in DNA synthesis (Figure 2B and data not shown). As both mutations were designed to be mostly isosteric in comparison to the wild-type residues, impaired DNA synthesis of the single mutants may derive from the hydrophobic nature of the mutant residues. Loss of either of the two polar interactions could lead to distortion of structural coordination within the motifs YGDTDS and KXY. Indeed, impaired DNA synthesis in such mutants is attributed to the reduced ability to stabilize primer/template complexes at the DNA polymerase active site [29, 30]. Combination of both mutations in one enzyme (mutant M2) results in an enzyme exhibiting half of the wild-type activity. A rationale for this could be that structural coordination of the motifs YGDTDS and KXY is somewhat restored by hydrophobic interactions between L541 and M593 in a tight pocket of the enzyme.

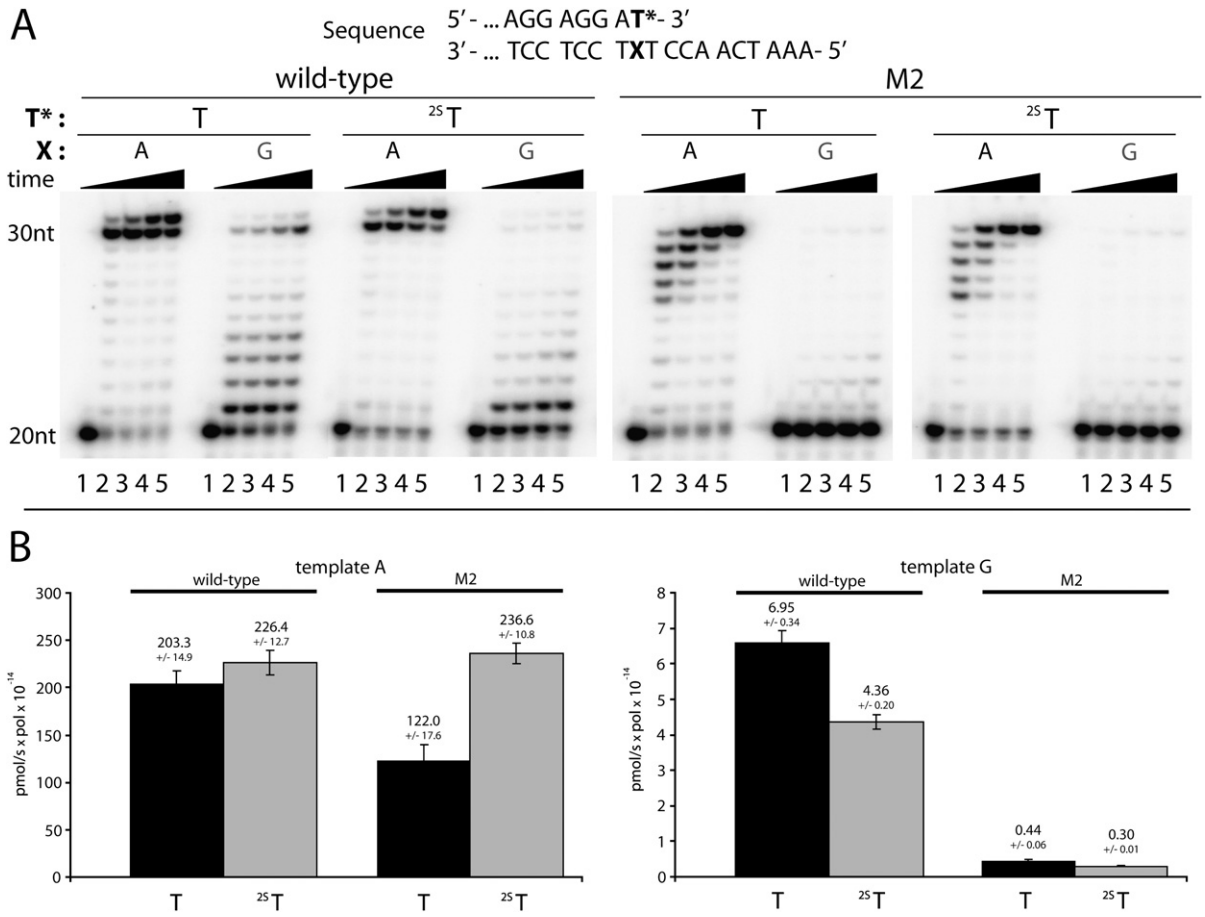

Figure 4. Increase of Mismatch Extension Fidelity through Single-Atom Substitution and Hydrophobic Substitution Mutation

(A) Time course of primer extension reactions conducted with the indicated enzyme and nonmodified (T) and thiolated (^{2S}T) primer strands under otherwise identical reaction conditions. Reactions were stopped at 0, 2, 16, 30, and 60 min (lanes 1–5), respectively. Primer/template constructs resulting in matched (X = A) and mismatched (X = G) complexes were employed as indicated. The first lane of each set represents a control without enzyme.

(B) Histograms of steady-state turnover rates on matched (template A) and mismatched (template G) primer/template complexes. Steady-state turnover rates were obtained for nonmodified (T) and thiolated (^{2S}T) primer strands under otherwise identical reaction conditions. The presented data derive from averages of independent experiments repeated at least three times.

It has recently been proposed that when encountering a mismatch, DNA polymerases actively misalign catalytic residues in the active site and, by that, reduce the enzymes catalytic proficiency [35]. The enhanced selectivity of mutant M2 could therefore derive from a more efficient active misalignment when encountering a mismatched primer/template caused by a destabilized active site. On the other side, the discussed Asp-Lys primer bridge in the wild-type enzyme might be able to stabilize a mismatched primer/template complex more efficiently than the hydrophobic substitution mutant M2. Even mismatches in the primer/template, which are located distal to the 3′-primer terminus, cause distortions [14, 36, 37] of the DNA enzyme complex that are sensed by the interaction of motif C (Figure 3). Additionally, although only slightly enhanced, the misinsertion selectivity displayed by mutant M2 suggests involvement of motif C in insertion fidelity.

In order to further substantiate the relevance of tight fitting, substrate geometry, and hydrogen-bonding networks for accurate and efficient primer extension, we altered the size and hydrogen-bonding capability of the primer substrate through substitution of a carbonyl group by thiocarbonyl (Figure 1D). Akin to results obtained through investigation of ^{2S}T insertion [38], thiolation of a primer/template complex at the depicted position (Figure 1D) causes an increase in selectivity and activity. As recently reported by Sintim and Kool, 2-thiothymidines in DNA duplexes results in an increased stability and hybridization selectivity [38]. As mentioned above, loss of the Asp-Lys primer bridge might destabilize the active site of mutant M2. In comparison to the wild-type, the more pronounced effect of the 2-thiothymidine modification on the turnover rate of mutant M2 could therefore derive from the increased stability of the primer/template complex employed. Furthermore, it has been shown

Table 1. Steady-State Analyses for Nucleotide Triphosphate Insertion and Misinsertion opposite a Template T

DNA Polymerase	Wild-Type			M2		
Inserted Nucleotide	K_M (μM)	V_{max} (min^{-1})	Efficiency V_{max}/K_M	K_M (μM)	V_{max} (min^{-1})	Efficiency V_{max}/K_M
dATP	0.16 ± 0.09	85.94 ± 11.93	554.43	0.09 ± 0.04	20.12 ± 2.14	226.03
dGTP	38.16 ± 11.12	18.90 ± 1.32	0.49	n.a.	n.a.	n.a.
dCTP	8.70 ± 2.53	4.59 ± 0.27	0.53	10.27 ± 3.67	1.45 ± 0.09	0.14
dTTP	21.40 ± 7.75	36.98 ± 2.61	1.73	n.a.	n.a.	n.a.

n.a., not accessible. Only negligible amounts of nucleotide insertions (<1%) were observed when up to 10 nM mutant M2 and up to 1.2 mM (higher dNTP concentrations cause inhibition of reaction) of the corresponding dNTP were applied. The presented data derive from averages of independent experiments repeated at least three times.

that, for example, *E. coli* DNA polymerase I (Klenow fragment) shows a kinetic preference for certain base analogs with increased sizes compared to the natural ones [39]. The slightly increased size of 2-thiothymidine could therefore additionally account for the enhanced turnover rates of both wild-type and mutant M2. As recently described, 2-thiothymidine/G mispairing was significantly suppressed [38]. Taking into account that a T/G mismatch builds a wobble base pair conformation in the active site of a family A DNA polymerase [36], the 2-thio modification possibly destabilizes this conformation through its increased sterical demand and lowered H-bonding capability. Although no such structural information is available for family B DNA polymerases, our results suggest this as

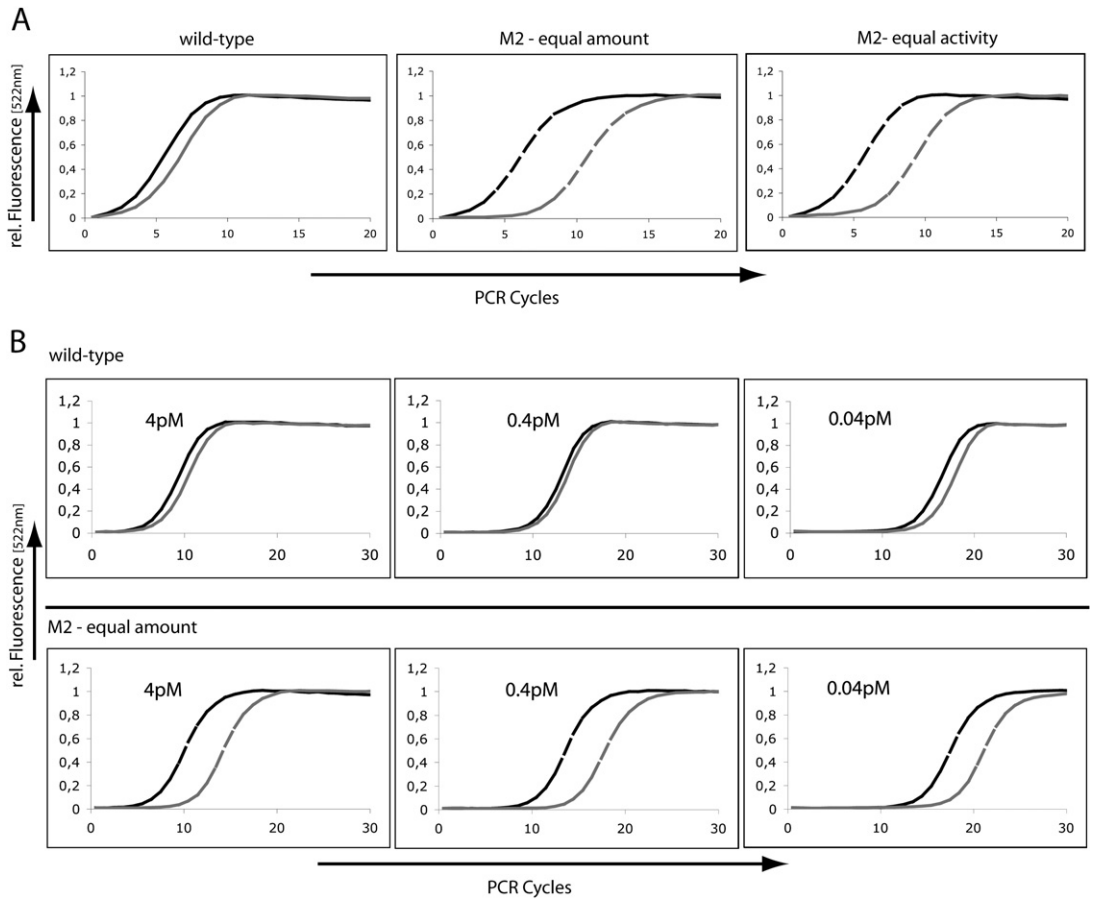

Figure 5. Real-Time PCR Experiments with Equal Amount and Equal Activity of *Pfu* DNA Polymerases and Template Dilutions Series

(A) Wild-type and mutant M2 at equal concentrations (20 nM, two left panels) and 40 nM of mutant M2 for equal activity.

(B) Real-time PCR experiments with template dilutions and equal amounts of *Pfu* DNA polymerases (20 nM). All reactions included 0.5 μM of each primer, 200 μM dNTPs, 0.4 × SybrGreen, and 40 pM template FarA (black) or FarG (gray) or dilutions thereof as depicted in the figure, respectively.

a possible mechanism for the enhanced mismatch extension fidelity when employing 2-thiothymidine modified primers.

Besides giving new insights into DNA polymerase fidelity mechanisms, the developed systems could find immediate application, for example, in advancement of genotyping methods [26, 40, 41]. The merit along this line of mutant M2 is the identification of a single nucleotide variation by allele-specific real-time PCR (Figure 5). In this method, signal generation relies on the tolerance of the mutant to the presence of SYBRgreen. These improved properties are evidenced by comparing amplification curves resulting from matched and mismatched primer/template complexes (Figure 5). In terms of these methods, single nucleotide variation diagnostics are feasible only if the double mutant is employed. This makes mutant M2 readily available for needs in efficient genotyping.

Additionally, it has been recently shown that DNA polymerase selectivity is directly linked to diseases like cancer [42, 43]. In some cancer cell lines, mutated DNA polymerases were found that exhibit lower selectivity than the wild-type enzymes [42]. Eukaryotic DNA polymerases that catalyze most of the DNA synthesis during replication exhibit the same sequence motifs as the herein-investigated enzyme [29, 30]. Thus, the depicted results might provide a rationale to increase the selectivity of these enzymes and study the effects on cell proliferation. So far, the herein-depicted amino acid substitutions have been studied exclusively. It remains to be elucidated whether other amino acid combinations at the respective positions may cause the similar effects as found for M2.

SIGNIFICANCE

Fidelity mechanisms of DNA polymerases are not fully understood. This study investigates the role of a highly conserved DNA polymerase motif for DNA polymerase selectivity. Our results give new insights into fidelity mechanisms of family B high-fidelity DNA polymerases and describe for the first time, to our knowledge, the increase of the selectivity of a family B DNA polymerase. The impact of rationally designed hydrophobic substitution mutations of a distinct polar interaction with the DNA template and single-atom replacement in the DNA template has been investigated. These modifications result in systems with higher selectivity. Our results are in conformity with findings for family A DNA polymerases and suggest a common mechanism. Furthermore, the hypothesis for motif C being a common mismatch sensor in DNA polymerases is supported as well as the relevance of hydrogen bonding, in addition to shape, for DNA polymerase selectivity highlighted. The combination of biological and chemical alterations leading to a more selective system has not been shown before, and the increased mismatch extension selectivity of developed systems may find applications, for example, in advancement of methods for genotyping such as allele-specific PCR. Additionally, it has been recently shown that diseases like cancer are directly linked to DNA polymerase selectivity. Mutated DNA polymerases found in some cancer cell lines exhibit lower selectivity in comparison to the respective wild-type enzymes. Major parts of replicative DNA synthesis are catalyzed by eukaryotic DNA polymerases that exhibit the same sequence motifs as the herein-investigated enzyme. Thus, the depicted results might provide a rationale to increase the selectivity of these enzymes and study the effects on cell proliferation.

EXPERIMENTAL PROCEDURES

Pfu DNA Polymerase Mutation, Expression, and Purification

All *Pfu* DNA polymerases carried two amino acid replacements, D141A and E143A, which eliminate the 3′-5′ exonuclease activity. Mutant phenotypes D541L and K593M were introduced into the *Pfu* DNA polymerase ORF via the QuikChange method (Stratagene) with the following primers: *Pfu*-L541QC1, 5′-d(GGA TTT AAA GTC CTC TAC ATT TTA ACT GAT GGT CTC TAT GC)-3′; *Pfu*-L541QC2, 5′-d(GCA TAG AGA CCA TCA GTT AAA ATG TAG AGG ACT TTA AAT CC)-3′; *Pfu*-M593QC1, 5′-d(GGA TTC TTC GTT ACG AAG ATG AGG TAT GCA GTA ATA G)-3′; and *Pfu*-M593QC2, 5′-d(CTA TTA CTG CAT ACC TCA TCT TCG TAA CGA AGA ATC C)-3′. Expression of all *Pfu* DNA polymerases (in pET*Pfu*) was conducted in *E. coli* BL21 (DE3) p*LysS*. Expression cultures were inoculated with 2% of an overnight culture grown at 30°C, and expression was induced at OD_{600} = 0.5 with IPTG at a final concentration of 1 mM. After 4 hr of expression, cultures were centrifuged at 5300 × g for 30 min. All cultures were grown in LB medium (Roth) with 34 ng/μl kanamycin and 34 ng/μl chloramphenicol. Collected cell pellets were resuspended in lysis-buffer (10 mM Tris-HCl [pH 9.55], 300 mM NaCl, 0.1% Triton X-100, 1 mM benzamidine, 1 mM Pefabloc [Roth], 1 mg/ml lysozyme, 5 ml lysis buffer/50 ml culture) and lysed at 37°C for 10 min. *E. coli* proteins were denaturated through heating to 75°C for 45 min with a subsequent centrifugation at 25,000 × g for 30 min at 4°C. Centrifuged expression lysates were incubated with pre-equilibrated (in 10 mM Tris-HCl [pH 9.55], 0.3 M NaCl, 0.1% Triton X-100) NTA-matrix (QIAGEN, 2–3 ml slurry/20 ml lysate) for 20 min at 4°C in an overhead shaker. The NTA matrix was then washed twice with NTA-wash-buffer (10 mM Tris-HCl [pH 8.1], 100 mM NaCl, 0.1% Triton X-100, 20 mM imidazole), and protein was eluted twice with NTA-elution-buffer (10 mM Tris-HCl [pH 8.1], 100 mM NaCl, 0.1% Triton X-100, 150 mM imidazole).

Resulting protein solutions were applied to a Sephacryl S-300 High Resolution (Amersham) column, pre-equilibrated with 150 mM Tris-HCl (pH 8.2) and 0.3 mM EDTA in order to exchange buffer and remove imidazole and residual protein impurities. Fractions containing *Pfu* DNA polymerase were pooled and 20× concentrated by VIVASPIN 20 50000 MWCO PES. Purified DNA polymerases were stored in *Pfu* storage buffer (50 mM Tris-HCl [pH 8.2], 0.1 mM EDTA, 1 mM DTT, 0.05% CHAPS, 50% glycerol) and were >95% pure as verified by SDS-PAGE. Protein concentrations were measured via the Bradford assay (Roth) with a BSA-standard (PIERCE albumin standard) curve.

PCR Experiments

PCR experiments were conducted in an overall volume of 50 μl. Reactions included 10 ng template (pET*Pfu* WT exo−) [44] in *Pfu* reaction buffer (20 mM Tris-HCl [pH 8.8 at 25°C], 2 mM $MgSO_4$, 10 mM $[NH_4]_2SO_4$, 10 mM KCl, 0.1% [v/v] Triton X-100, 0.1 mg/ml BSA). Final enzyme concentration in all reactions was 150 nM with dNTPs (200 μM each) and primers (0.2 μM each): primer 1, 5′-d(GGT ATT GAG GGT CGC ATG ATT TTA GAT GTG GAT TAC ATA ACT G)-3′; primer 2, 5′-d(AGA GGA GAG TTA GAG CCC TAG GAT TTT TTA ATG TTA AGC CAG GAA G)-3′. The following cycle program was applied: 95°C 1 min and then 25 cycles with 95°C for 1 min, 55°C for 1 min, 72°C for 3 min, and a final elongation step at 72°C for 5 min. Reaction

products were separated on a 0.8% agarose gel and stained with ethidium bromide (Figure 2A).

Primer Extension Assays

Primer/template substrates were annealed by mixing 5′-^{32}P-labeled primer and template in *Pfu* DNA polymerase reaction buffer (20 mM Tris-HCl [pH 8.8], 10 mM $[NH_4]_2SO_4$, 10 mM KCl, 0.1% Triton X-100, 0.1 mg/ml BSA, 2 mM $MgSO_4$). The mixture was heated to 95°C for 5 min and subsequently cooled down to 20°C over 30 min. After annealing, reactions were initiated by addition of 10 μl enzyme and dNTP solution in 1× reaction buffer to 10 μl annealing mix. All reactions were incubated at 68°C for 5 min, including 22.5 nM of each enzyme, 200 μM dATP only (Figure 2C), or 200 μM of each dNTP (Figure 2D) and 150 nM primer/template complex. Sequences for the Figure 2C: primer FT20T (5′-d[CGT TGG TCC TGA AGG AGG AT]-3′) and template strand F33A (X: A) (5′-d[AAA TCA ACC TXT CCT CCT TCA GGA CCA ACG TAC]-3′), F33G (X: G), F33C (X: C), and F33T (X: T). Sequences for Figure 2D: FT20T and F33A, respectively. After incubation, reactions were quenched by addition of two reaction volumes of gel-loading buffer (80% formamide, 20 mM EDTA), and product mixtures were analyzed by 12% denaturating PAGE with subsequent phosphorimager analysis (Figures 2C and 2D).

Primer Extension Assays—Time Course

These primer extension reactions (Figure 4A) were conducted as described in Primer Extension Assays including the following alterations. The reactions were quenched after incubation for the indicated time (0, 2, 16, 30, 60 min) and comprised 60 nM of each enzyme, 100 μM of each dNTP, and 150 nM primer/template complex. Sequences: primer FT20T or FT202ST (5′-d[CGT TGG TCC TGA AGG AGG A^{2S}T]-3′) and ^{2S}T: 2-thiothymidine residue, respectively. Template strands: F33A or F33G, respectively.

DNA Polymerase Activity Determination

Primer/template (FT20T/F33A) complexes were annealed, and the reaction initiated described in Primer Extension Assays. The reactions contained varying enzyme amounts (1–80 nM), 100 μM dNTPs, and 150 nM primer/template complex. After incubation for 10 min at 68°C, reactions were quenched by addition of two reaction volumes of gel-loading buffer (80% formamide, 20 mM EDTA), and product mixtures were analyzed by 12% denaturating PAGE. Activity was measured by quantifying the intensity of each band produced by the respective DNA polymerase with a Phosphorimager. From this quantification, the amount of incorporated nucleotides was calculated. The total amount of incorporated nucleotides for each reaction equals the sum of incorporated nucleotide of each band. The presented results (Figure 2B) are from measurements that were independently repeated at least three times.

Steady-State Mismatch Extension Kinetics

Primer/template (FT20T/F33A or F33G and FT202ST/F33A or F33G, respectively) complexes were annealed and the reaction initiated as in Primer Extension Assays. The reactions contained 100 μM dNTPs and 150 nM primer/template complex, at given enzyme amounts (0.5–75 nM). The reactions were incubated at 68°C, quenched after varying time intervals (2–120 min) by addition of two reaction volumes of gel-loading buffer (80% formamide, 20 mM EDTA). Product mixtures were analyzed by 12% denaturating PAGE. Activity was measured by quantifying the intensity of each band produced by the respective DNA polymerase with a phosphorimager. From this quantification, the amount of incorporated nucleotides per time was calculated. The total amount of incorporated nucleotides for each reaction equals the sum of incorporated nucleotide of each band. The presented results (Figure 4B) are from measurements that were independently repeated at least three times.

Steady-State Insertion Kinetics

The primer/template (FT20T/F33A) complex was annealed and the reaction initiated as described in Primer Extension Assays. The reactions contained varying amounts of dATP, dGTP, dCTP, or TTP (5 nM–1 mM) and 150 nM primer/template complex, with varying enzyme amounts (0.5–5 nM). The reactions were incubated at 68°C, quenched after varying time intervals (10–60 min) by addition of two reaction volumes of gel-loading buffer (80% formamide, 20 mM EDTA). Reaction conditions were adjusted for different reactions to allow 20% or less primer extension ensuring single completed hit conditions according to published procedures [45]. Product mixtures were analyzed by 12% denaturating PAGE, and data were quantified by phosphorimager analysis. The presented results (Table 1) are from measurements that were independently repeated at least three times.

Recognition of Remote Mismatches

Primer/template complexes (sequences as indicated in Figure 4) were annealed as described in Primer Extension Assays. After annealing, reactions were initiated by addition of 10 μl enzyme and dATP solution in 1× reaction buffer to 10 μl annealing mix. Assays included 200 μM dATP and 22.5 nM of each enzyme. Reactions were incubated at 68°C for 5 min. After incubation, reactions were quenched by addition of two reaction volumes of gel-loading buffer (80% formamide, 20 mM EDTA), and product mixtures were analyzed by 12% denaturating PAGE with subsequent phosphorimager analysis (Figure 3).

Synthesis of Oligonucleotides Containing ^{2S}T

2-Thio-5′-*O*-(4,4′-dimethoxytrityl)-thymidine (catalog number PY 7510) was purchased at Berry & Associates, Inc. DNA oligonucleotides were synthesized on a 0.2 μmol scale on an Applied Biosystems 392 DNA synthesizer, with commercially available 2-(cyanoethyl)phosphoramidites. A standard method for 2-(cyanoethyl)phosphoramidites was used, with the exception that the coupling times from the modified nucleotides were extended to 10 min. Yields for modified oligonucleotides were similar to those obtained for unmodified oligonucleotides. After synthesis (trityl off) the oligonucleotides were cleaved from the support by treatment with conc. NH_4OH at RT for 24 hr. Subsequently NH_4OH was removed, and the oligonucleotide was purified by preparative electrophoresis on a 12% polyacrylamide gel containing 8 M urea. DNA oligonucleotides were recovered by standard precipitation with ethanol in the presence of 0.3 M sodium acetate. The oligonucleotides were purified a second time by using RP-HPLC with 0.1 M triethylammonia acetate buffer (pH 7). Incorporation of ^{2S}T was also verified spectroscopically by the characteristic absorption band 277 nm. After removal of the solvent, the oligonucleotides were dissolved in water and quantified by absorption measurements at 260 nm. The integrity of all modified oligonucleotides was confirmed by MALDI-ToF (Metabion GmbH). MALDI-ToF MS: expected 6229.1, found 6234.4 for 5′-d(CGT TGG TCC TGA AGG AGG A^{2S}T)-3′.

Real-Time PCR Experiments

Real-time PCR was performed by using an iCycler (BIORAD) system. The reactions were performed in an overall volume of 20 μl containing 40 pM of the respective templates in *Pfu* DNA polymerase buffer (20 mM Tris-HCl [pH 8.8], 10 mM KCl, 10 mM $[NH_4]_2SO_4$, 2 mM $MgSO_4$, 0.1% Triton X-100, 0.1 mg/ml nuclease-free bovine serum albumin). The final mixtures contained dNTPs (200 μM each of dATP, dGTP, dCTP, and TTP), primers (0.5 μM each of respective primer probe and reverse primer), 0.4× SybrGreen solution (Sigma), and *Pfu* DNA polymerases as indicated in the figures. PCR was performed employing the following program: initial denaturation at 95°C for 3 min followed by 40 cycles of denaturation at 95°C for 30 s, primer annealing at 55°C for 35 s, and extension at 72°C for 40 s. The presented results (Figure 5) are from at least three times repeated independent measurements of duplicates that originated from one master mix. DNA sequences applied: primer probe FT20T, reverse primer, 5′-d(CGC GCA GCA CGC GCC GCC GT)-3′; target template FarX, 5′-d(CCG TCA GCT GTG CCG TCG CGC AGC ACG CGC CGC CGT GGA

CAG AGG ACT GCA GAA AAT CAA CCT XTC CTC CTT CAG GAC CAA CGT ACA GAG)-3′; X: A, FarA; G, FarG.

ACKNOWLEDGMENTS

Financial support by the Volkswagen Foundation is gratefully acknowledged.

Received: October 17, 2006
Revised: November 28, 2006
Accepted: November 30, 2006
Published: February 23, 2007

REFERENCES

1. Kornberg, A., and Baker, T. (1992). DNA Replication (New York: Freeman).
2. Echols, H., and Goodman, M.F. (1991). Fidelity mechanisms in DNA replication. Annu. Rev. Biochem. *60*, 477–511.
3. Goodman, M.F. (1997). Hydrogen bonding revisited: geometric selection as a principal determinant of DNA replication fidelity. Proc. Natl. Acad. Sci. USA *94*, 10493–10495.
4. Kool, E.T. (2002). Active site tightness and substrate fit in DNA replication. Annu. Rev. Biochem. *71*, 191–219.
5. Kunkel, T.A. (2004). DNA replication fidelity. J. Biol. Chem. *279*, 16895–16898.
6. Kunkel, T.A., and Bebenek, K. (2000). DNA replication fidelity. Annu. Rev. Biochem. *69*, 497–529.
7. Patel, P.H., and Loeb, L.A. (2001). Getting a grip on how DNA polymerases function. Nat. Struct. Biol. *8*, 656–659.
8. Beard, W.A., Osheroff, W.P., Prasad, R., Sawaya, M.R., Jaju, M., Wood, T.G., Kraut, J., Kunkel, T.A., and Wilson, S.H. (1996). Enzyme-DNA interactions required for efficient nucleotide incorporation and discrimination in human DNA polymerase beta. J. Biol. Chem. *271*, 12141–12144.
9. Minnick, D.T., Astatke, M., Joyce, C.M., and Kunkel, T.A. (1996). A thumb subdomain mutant of the large fragment of *Escherichia coli* DNA polymerase I with reduced DNA binding affinity, processivity, and frameshift fidelity. J. Biol. Chem. *271*, 24954–24961.
10. Polesky, A.H., Steitz, T.A., Grindley, N.D., and Joyce, C.M. (1990). Identification of residues critical for the polymerase activity of the Klenow fragment of DNA polymerase I from *Escherichia coli*. J. Biol. Chem. *265*, 14579–14591.
11. Spratt, T.E. (2001). Identification of hydrogen bonds between *Escherichia coli* DNA polymerase I (Klenow fragment) and the minor groove of DNA by amino acid substitution of the polymerase and atomic substitution of the DNA. Biochemistry *40*, 2647–2652.
12. Yang, G., Wang, J., and Konigsberg, W. (2005). Base selectivity is impaired by mutants that perturb hydrogen bonding networks in the RB69 DNA polymerase active site. Biochemistry *44*, 3338–3346.
13. Morales, J.C., and Kool, E.T. (1999). Minor groove interactions between polymerase and DNA: more essential to replication than Watson-Crick hydrogen bonds? J. Am. Chem. Soc. *121*, 2323–2324.
14. Summerer, D., and Marx, A. (2002). Differential minor groove interactions between DNA polymerase and sugar backbone of primer and template strands. J. Am. Chem. Soc. *124*, 910–911.
15. Doublie, S., Tabor, S., Long, A.M., Richardson, C.C., and Ellenberger, T. (1998). Crystal structure of a bacteriophage T7 DNA replication complex at 2.2 A resolution. Nature *391*, 251–258.
16. Franklin, M.C., Wang, J., and Steitz, T.A. (2001). Structure of the replicating complex of a pol alpha family DNA polymerase. Cell *105*, 657–667.
17. Huang, H., Chopra, R., Verdine, G.L., and Harrison, S.C. (1998). Structure of a covalently trapped catalytic complex of HIV-1 reverse transcriptase: implications for drug resistance. Science *282*, 1669–1675.
18. Johnson, S.J., Taylor, J.S., and Beese, L.S. (2003). Processive DNA synthesis observed in a polymerase crystal suggests a mechanism for the prevention of frameshift mutations. Proc. Natl. Acad. Sci. USA *100*, 3895–3900.
19. Kiefer, J.R., Mao, C., Braman, J.C., and Beese, L.S. (1998). Visualizing DNA replication in a catalytically active Bacillus DNA polymerase crystal. Nature *391*, 304–307.
20. Li, Y., Korolev, S., and Waksman, G. (1998). Crystal structures of open and closed forms of binary and ternary complexes of the large fragment of Thermus aquaticus DNA polymerase I: structural basis for nucleotide incorporation. EMBO J. *17*, 7514–7525.
21. Li, Y., and Waksman, G. (2001). Crystal structures of a ddATP-, ddTTP-, ddCTP, and ddGTP-trapped ternary complex of Klentaq1: insights into nucleotide incorporation and selectivity. Protein Sci. *10*, 1225–1233.
22. Pelletier, H., Sawaya, M.R., Wolfle, W., Wilson, S.H., and Kraut, J. (1996). Crystal structures of human DNA polymerase beta complexed with DNA: implications for catalytic mechanism, processivity, and fidelity. Biochemistry *35*, 12742–12761.
23. Seeman, N.C., Rosenberg, J.M., and Rich, A. (1976). Sequence-specific recognition of double helical nucleic acids by proteins. Proc. Natl. Acad. Sci. USA *73*, 804–808.
24. Loh, E., and Loeb, L.A. (2005). Mutability of DNA polymerase I: implications for the creation of mutant DNA polymerases. DNA Repair (Amst.) *4*, 1390–1398.
25. Minnick, D.T., Bebenek, K., Osheroff, W.P., Turner, R.M., Jr., Astatke, M., Liu, L., Kunkel, T.A., and Joyce, C.M. (1999). Side chains that influence fidelity at the polymerase active site of *Escherichia coli* DNA polymerase I (Klenow fragment). J. Biol. Chem. *274*, 3067–3075.
26. Summerer, D., Rudinger, N.Z., Detmer, I., and Marx, A. (2005). Enhanced DNA polymerase mismatch extension fidelity by directed combinatorial enzyme design. Angew. Chem. Int. Ed. Engl. *44*, 4712–4715.
27. Braithwaite, D.K., and Ito, J. (1993). Compilation, alignment, and phylogenetic relationships of DNA polymerases. Nucleic Acids Res. *21*, 787–802.
28. Delarue, M., Poch, O., Tordo, N., Moras, D., and Argos, P. (1990). An attempt to unify the structure of polymerases. Protein Eng. *3*, 461–467.
29. Blasco, M.A., Mendez, J., Lazaro, J.M., Blanco, L., and Salas, M. (1995). Primer terminus stabilization at the phi 29 DNA polymerase active site. Mutational analysis of conserved motif KXY. J. Biol. Chem. *270*, 2735–2740.
30. Copeland, W.C., and Wang, T.S. (1993). Mutational analysis of the human DNA polymerase alpha. The most conserved region in alpha-like DNA polymerases is involved in metal-specific catalysis. J. Biol. Chem. *268*, 11028–11040.
31. Biles, B.D., and Connolly, B.A. (2004). Low-fidelity *Pyrococcus furiosus* DNA polymerase mutants useful in error-prone PCR. Nucleic Acids Res. *32*, e176.
32. Cline, J., Braman, J.C., and Hogrefe, H.H. (1996). PCR fidelity of pfu DNA polymerase and other thermostable DNA polymerases. Nucleic Acids Res. *24*, 3546–3551.
33. Fogg, M.J., Pearl, L.H., and Connolly, B.A. (2002). Structural basis for uracil recognition by archaeal family B DNA polymerases. Nat. Struct. Biol. *9*, 922–927.
34. Connolly, B.A. (1992). Synthetic oligodeoxynucleotides containing modified bases. Methods Enzymol. *211*, 36–53.

35. Tsai, Y.C., and Johnson, K.A. (2006). A new paradigm for DNA polymerase specificity. Biochemistry *45*, 9675–9687.

36. Johnson, S.J., and Beese, L.S. (2004). Structures of mismatch replication errors observed in a DNA polymerase. Cell *116*, 803–816.

37. Strerath, M., Gaster, J., and Marx, A. (2004). Recognition of remote mismatches by DNA polymerases. ChemBioChem *5*, 1585–1588.

38. Sintim, H.O., and Kool, E.T. (2006). Enhanced base pairing and replication efficiency of thiothymidines, expanded-size variants of thymidine. J. Am. Chem. Soc. *128*, 396–397.

39. Kim, T.W., Delaney, J.C., Essigmann, J.M., and Kool, E.T. (2005). Probing the active site tightness of DNA polymerase in subangstrom increments. Proc. Natl. Acad. Sci. USA *102*, 15803–15808.

40. Strerath, M., and Marx, A. (2005). Genotyping—from genomic DNA to genotype in a single tube. Angew. Chem. Int. Ed. Engl. *44*, 7842–7849.

41. Syvanen, A.C. (2001). Accessing genetic variation: genotyping single nucleotide polymorphisms. Nat. Rev. Genet. *2*, 930–942.

42. Sweasy, J.B., Lang, T., Starcevic, D., Sun, K.W., Lai, C.C., Dimaio, D., and Dalal, S. (2005). Expression of DNA polymerase {beta} cancer-associated variants in mouse cells results in cellular transformation. Proc. Natl. Acad. Sci. USA *102*, 14350–14355.

43. Venkatesan, R.N., Hsu, J.J., Lawrence, N.A., Preston, B.D., and Loeb, L.A. (2006). Mutator phenotypes caused by substitution at a conserved motif A residue in eukaryotic DNA polymerase delta. J. Biol. Chem. *281*, 4486–4494.

44. Dabrowski, S., and Kur, J. (1998). Cloning and expression in *Escherichia coli* of the recombinant his-tagged DNA polymerases from *Pyrococcus furiosus* and *Pyrococcus woesei*. Protein Expr. Purif. *14*, 131–138.

45. Creighton, S., Bloom, L.B., and Goodman, M.F. (1995). Gel fidelity assay measuring nucleotide misinsertion, exonucleolytic proofreading, and lesion bypass efficiencies. Methods Enzymol. *262*, 232–256.

